ELSEVIER

Journal of Photochemistry and Photobiology A: Chemistry 126 (1999) 77–82

Journal of Photochemistry and Photobiology A:Chemistry

www.elsevier.nl/locate/jphotochem

Fluorescence anisotropy of dyes included in crosslinked polystyrene

Marcia Levitus [a], José Luis Bourdelande [b,1], Gerard Marqués [b,2], Pedro F. Aramendía [a,*]

[a] *INQUIMAE, Departamento de Química Inorgánica, Analítica y Química Física, Facultad de Ciencias Exactas y Naturales, Universidad de Buenos Aires, Pabellón 2, Ciudad Universitaria, 1428 Buenos Aires, Argentina*

[b] *Unitat de Química Orgànica, Departament de Química, Universitat Autònoma de Barcelona, Bellaterra, 08193 Barcelona, Spain*

Accepted 26 May 1999

Abstract

In this work we investigate on the local free volume of a crosslinked polystyrene by studying the steady-state fluorescence anisotropy of three probes with different sizes and shape, embedded in the polymer matrix. The very low values measured for the steady-state fluorescence anisotropy show that the molecules can perform ample movements during their excited-state lifetimes (typically few nanoseconds). Moreover, anisotropy values decrease with the size of the probe. Results were interpreted in terms of Saupe order parameters and the wobbling-in-cone model. ©1999 Elsevier Science S.A. All rights reserved.

Keywords: Fluorescence; Anisotropy; Polystyrene

1. Introduction

The dependence of fluorescence anisotropy upon rotational diffusion resulted in numerous applications in studies of dynamics of macromolecular systems. Fluorescence polarization has been extensively used in molecular biology for studying processes such as protein–ligand association, protein denaturation, and for studying properties such as internal viscosity and mobility of membranes [1].

In the synthetic polymer field, only a limited number of studies have been carried out with this technique, in spite of its real potential for studying polymer dynamics. Many of the applications involving polymers study the distribution of molecular orientations in partially ordered systems in which there is negligible motion of the fluorescent molecule during its excited-state lifetime. In this case, it is possible to obtain second-order orientation averages as well as fourth-order averages, giving an insight into the distribution of molecular orientations [2,3].

In isotropic media, covalently bound fluorescent probes can give information about mobility of chain segments, occurring either in polymer solutions or in bulk polymers [4,5].

On the other hand, chromophores dispersed in the medium can give information on the local free volume accessible to the probe. This was studied by total fluorescence emission or by isomerization [6–8]. Molecular rotation involves comparable volumes as isomerization for the motion, and is thus equally capable of detecting such volume requirements. The difference is the timescale in which the different movements take place.

Besides, in the area of solid phase synthesis it is difficult to characterize the structure of a polymer once a reactant has been covalently linked to the skeleton: as they are solid many of the usual analytical methods are unsuitable [9,10]. The reactivity of the new polymeric equivalent of the reactant depends on the macromolecular environment. Gaining insight on this environment can help to understand such reactivity.

In this work we investigate the local free volume of a crosslinked polystyrene by studying the fluorescence anisotropy of three fluorescent probes differing in shape and size which are dispersed in the polymer network. The three probes used were chosen considering their high fluorescence quantum yield and high maximum fluorescence anisotropy, and taking into account that their absorption and fluorescence spectra do not overlap with the absorption spectrum of the polymer. Their structure are shown in Fig. 1.

* Corresponding author. Fax: +54-11-4576-3341

E-mail addresses: iqor2@cc.uab.es (J. Bourdelande), iqor2@cc.uab.es (G. Marqués), pedroa@ql.fcen.uba.ar (P.F. Aramendía)

[1] Fax: +34-93-581-1265.

[2] Fax: +34-93-581-1265.

PII: S1010-6030(99)00125-2

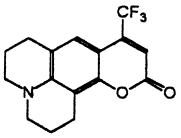

Coumarin 153

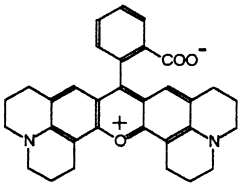

Rhodamine 101

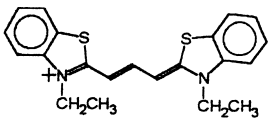

DTCI

Fig. 1. Structures of the dye molecules.

2. Experimental

2.1. Chemicals

All probes, Rhodamine 101 (inner salt, Kodak), coumarin 153 (laser grade, Kodak) and 3,3′-diethyl thiadicarbocyanine iodide (DTCI) (laser grade, Lambda Physik) were used as received. (see Fig. 1 for molecular structures).

Solvents, dichloromethane (HPLC grade), methanol (analytical grade) and glycerol (analytical grade) were used without further purification.

The polystyrene used was a (98 : 2) copolymer of styrene–divinylbenzene, 200–400 mesh, purchased from Eastman-Kodak. Prior to its use, polystyrene (150 g) was sequentially washed with: ethanol–dioxane–water (30 : 4 : 1, v/v/v), 5 l; ethanol, 300 ml; ethanol–dioxane (2 : 1) 300 ml; ethanol–dioxane (1 : 1) 300 ml; dioxane 1 l; dioxane–ether (1 : 1) 500 ml; dioxane–ether (1 : 2) 500 ml; and ether 1 l. Dried (80°C, 2 Torr) to constant weight (149.5 g) over P_2O_5.

2.2. Preparation of samples

Around 0.5 g of polystyrene-co-2% divinylbenzene as powder was suspended in a solution of the probe in dichloromethane (a solvent that swells the polymer). The ratio probe to polymer in the mixture was always less than 0.2% (w/w). The suspension was stirred in a 25 ml round-bottomed flask for 30 h in the dark, at room temperature, then filtered and extensively washed with methanol (a solvent that does not swell the polymer) until the washing aliquot was colorless. In this way the probe placed initially on the surface is completely removed. The sample was finally dried overnight in a vacuum oven at room temperature.

Samples were grained prior to use to ensure a homogeneous packing in the cuvette.

2.3. Luminescence measurements

Steady-state excitation, emission and fluorescence anisotropy spectra were recorded with a PTI Quantamaster spectrofluorimeter provided with polarizers. Solid samples were measured with front-face configuration (excitation at 30° with respect to the normal of the surface, emission at 90° with respect to excitation) in a 0.1 mm path quartz cuvette placed in a thermostatizable cell holder. An optical filter with transmittance lower than 0.5% at the excitation wavelength was placed before the emission slit to attenuate scattered light. Measurements were made at room temperature and at 60°C.

The steady-state anisotropy, $\langle r(\lambda)\rangle$, was calculated at each emission wavelength as

$$\langle r(\lambda)\rangle = \frac{I_{VV}(\lambda) - I_{VH}(\lambda)G(\lambda)}{I_{VV}(\lambda) + 2I_{VH}(\lambda)G(\lambda)}, \qquad G = \frac{I_{VH}(\lambda)}{I_{HH}(\lambda)} \quad (1)$$

$I(\lambda)$ represent the wavelength dependent intensity and the subscripts V and H have the usual meaning in anisotropy measurements [11]: they denote the orientation of the linearly polarized E vector of radiation on the excitation and emission beams, respectively. The subscript V denotes polarization perpendicular to the plane of incidence, while H denotes polarization parallel to this plane.

The G factor corrects for the different sensitivities of the optical elements of the spectrofluorimeter to the polarization direction of the light. When the value of the maximum fluorescence anisotropy, r_0, was not available from literature, it was obtained from measurements in glycerol 87% v/v in water performed between 10 and −10°C in a 10 mm path quartz cuvette with 90° configuration.

To check for the influence of multiple reflections in the polymer matrix, on the polarization of the probe emission, we prepared a set of samples of Rhodamine 101 having the same probe concentration but lower values of diffuse reflectance, R, than the sample in the 0.1 mm path cuvette described above. Samples with small R values were prepared by sticking a very thin layer of solid on a piece of black paper by means of double stick tape. Fluorescence anisotropy of these samples was measured replacing the 0.1 mm path cuvette by this piece of paper.

Samples with intermediate R values were prepared in a 0.01 mm path quartz cuvette. Diffuse reflectance was measured in a Shimadzu 3101-PC UV–VIS spectrophotometer provided with an integrating sphere.

2.4. Molecular modeling

Geometry optimization of the probe molecules was performed with the AM1 semiempirical method.

3. Results

Spectral distribution of both excitation and emission spectra of the three solid samples were identical to the ones measured for the same chromophores in dilute solution, indicating the absence of aggregates.

Front-face excitation is a requirement for non-transparent solid samples as the ones studied in this work. This instrumental geometry is subject to light scattering artifacts even when dilute liquid samples are measured. Scattered light is totally polarized ($\langle r \rangle = 1$) whereas the fluorescence of an isotropically oriented sample is partially depolarized ($-0.2 \leq \langle r \rangle \leq 0.4$) [11]. Even small proportions of light scattering can affect fluorescence anisotropy measurements appreciably, causing an increase of the measured anisotropy [12]. Since the magnitude of this increment depends on the fraction of scattered light with respect to the fluorescence intensity, the anisotropy spectrum has a minimum at the fluorescence maximum and tends to unity at both sides of the spectrum, where only scattered light contributes. The influence of light scattering on anisotropy measurements depends on the fluorescence quantum yield of the chromophore, its concentration in the medium, and on experimental conditions such as excitation and emission slit widths, and geometry. An optical filter before the emission slit decreases the fraction of stray light but does not eliminate the effect.

To check for the influence of scattering in the measured anisotropy, we measured the anisotropy of the same liquid solution using both a 0.1 mm path cuvette with front-face configuration (as described in the experimental section) and the usual configuration with a 10 mm path square cuvette.

For liquid samples, used as check, front-face configuration gave an anisotropy spectrum with a minimum located at the fluorescence maximum, while the 90° configuration gave an $\langle r \rangle$ value which was constant within a 100 mm range around the fluorescence maximum.

The minimum $\langle r \rangle$ value in the anisotropy spectrum obtained with front-face configuration was dependent on the slit widths of excitation and emission when the proportion of scattered light was high and tended to a constant value as this proportion decreased. The proportion of scattered light was measured as the ratio $F = I_{VV}(\lambda_{max} + 200\,nm)/I_{VV}(\lambda_{max})$ and was dependent on both excitation and emission slit widths.

The minimum $\langle r \rangle$ value reached as the F-ratio decreased was identical to the $\langle r \rangle$ value measured with the 90° configuration, indicating that the influence of light scattering was negligible.

Solid samples were measured at different combinations of excitation and emission slit widths, and the same behavior was observed; the measured $\langle r \rangle$ decreased as the F-ratio decreased, tending to a constant value was taken as the anisotropy of the sample free of scattering artifacts.

To check for the possible influence of energy transfer between two chromophore molecules, the samples were diluted by washing them with dichloromethane and then with methanol as described in the experimental section. Anisotropy values did not change after washing within experimental error, indicating that energy transfer is not important in our measurements.

We also investigated the influence of diffuse reflectance on the polarization of the probe emission. To achieve this, $\langle r \rangle$ was measured for Rhodamine 101 samples with R values at the excitation wavelength ranging from 6 to 40%. Results showed an increase in $\langle r \rangle$ with decreasing R: the sample contained in the 0.1 mm path cuvette had 40% of R with $\langle r \rangle = 0.04$ while the thin sample stuck on double stick tape had $R = 6\%$ and a value of $\langle r \rangle = 0.29$ was obtained following the slit width optimization procedure.

This difference does not necessary imply that the emission is depolarized as the diffuse reflectance of the sample increases, since samples with small R values have also a very weak fluorescence and very high levels of scattering. In fact, emission spectra of sample with 6% of R were superimposed on a very high dispersion band, whose contribution to the total emission signal was around 30% at the fluorescence maximum. This contribution was too high, making it impossible to minimize its influence on the measured $\langle r \rangle$ by selecting the optimum excitation and emission slit widths as described above for the samples contained in the 0.1 mm path cuvette. In order to eliminate the scattering contribution to $\langle r \rangle$ in this case, it was necessary to subtract from each of the four emission components (Eq. (1)) the blank obtained by exciting the double stick tape without sample under identical conditions. Spectra with and without sample were identical at both sides of the spectrum, where the probe does not emit. This fact shows that in our case, scattering was due mainly to the paper and tape, and the influence of the very thin layer of solid was negligible. If it were not the case, a sample of polymer without probe should be used instead. Nevertheless, this procedure is not totally reliable since the light absorbed by the chromophore decreases the intensity of scattered light in sample with respect to the blank [12]. It is also difficult to prepare a blank of the same thickness and compactness as the matrix in the sample.

The steady-state anisotropy spectrum of the thin sample once the blank was subtracted showed a constant value, $\langle r \rangle = 0.04$, 20 nm around the fluorescence maximum. This $\langle r \rangle$ value coincides within experimental error with one measured in the sample with $R = 40\%$ (see below), where scattering artifacts were made negligible by selecting optimum slits.

These results show that, in our case, the light emitted by the probe is not further depolarized by diffuse reflectance. The high $\langle r \rangle$ values obtained with samples having low R values are a consequence of scattering artifacts.

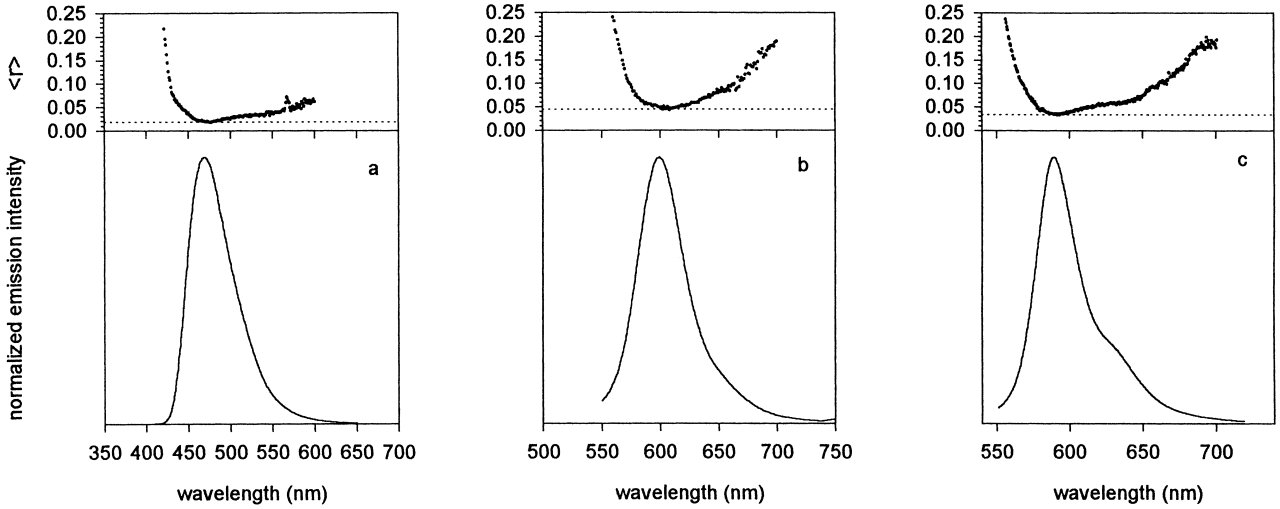

Fig. 2. Steady-state emission and fluorescence anisotropy spectra of (a) Coumarin 153; (b) Rhodamine 101; (c) DTCI in polystyrene-co-2% divinylbenzene. Excitation wavelengths were: a: 400 nm; b: 530 nm; c: 530 nm. Equal results are obtained at 25 and 60°C.

Table 1
Fluorescence lifetimes, τ_f; steady-state fluorescence anisotropy, $\langle r \rangle$; maximum fluorescence anisotropy, r_0; Saupe order parameter (see text), S; and wobbling-in-cone model semiangle (see text), θ_0 for the three samples studied. Results are temperature independent

	τ_f (ns)	$\langle r \rangle$	r_0	S[a]	θ_0[b]
Coumarin	~5[c]	0.018 ± 0.003	0.375[d]	0.22 ± 0.02	$71° \pm 1°$
DTCI	0.3[e]	0.033 ± 0.003	0.370[f]	0.30 ± 0.01	$65° \pm 1°$
Rhodamine 101	5.2[g]	0.044 ± 0.003	0.365	0.35 ± 0.01	$62° \pm 1°$

[a] Assuming $\langle r \rangle = r_\infty$ (see text).
[b] According to the Wobbling-in-cone model of Eq. (7) and Fig. 4 (see text).
[c] Average value in all common solvents. From [16].
[d] Value corresponding to excitation at 400 nm. From [14].
[e] Calculated as ϕ_f/k_f in ethanol at 25°C. From [13].
[f] From [13].
[g] Independent on solvent and temperature. From [17].

Fig. 2 shows fluorescence emission and anisotropy spectra of the three solid samples measured in a 0.1 mm path cuvette, where it was always possible to make scattering artifacts negligible by selecting optimum slits.

Anisotropy spectra and $\langle r \rangle$ were independent of temperature in the range studied. Maximum fluorescence anisotropy of Rhodamine 101 was obtained from measurements in glycerol at low temperatures. The anisotropy of this sample increased with decreasing temperature reaching a plateau at $\langle r \rangle = 0.365$, which was taken as r_0. For DTCI and Coumarin 153, r_0 values were obtained from literature [13,14].

The anisotropies measured for each sample are listed in Table 1 together with the corresponding r_0 values of each chromophore. It is possible to observe a correlation between $\langle r \rangle$ values and molecular size of the chromophores. The smallest molecule, Coumarin 153, gives the smallest anisotropy, while Rhodamine 101 gives the largest. Fig. 3 shows the minimized molecular geometry of the three probes in the same scale for size comparison.

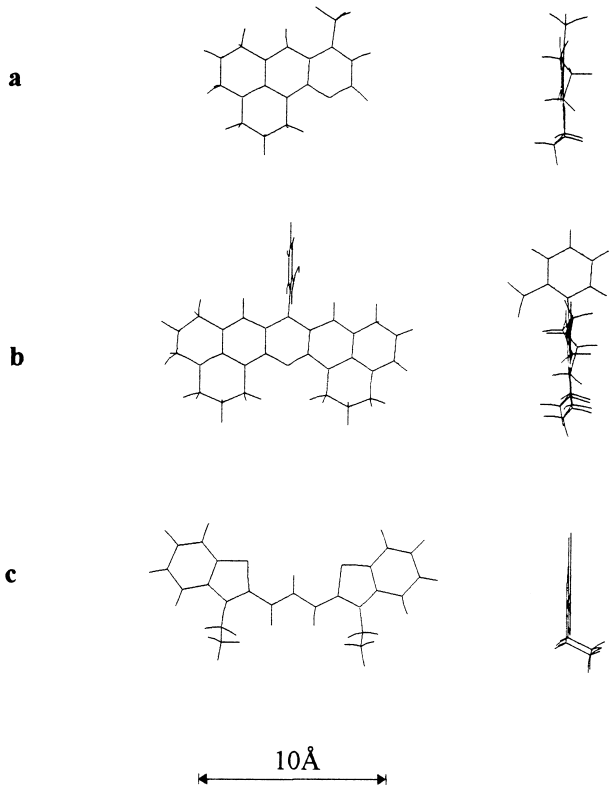

Fig. 3. Two perpendicular views of the minimized geometry of the three chromophores. (a) Coumarin 153, (b) Rhodamine 101, (c) DTCI. The thickness of aromatic rings are not shown.

4. Discussion

Steady-state anisotropies are the result of molecular rotation of excited molecules. The probes used in this work have a very high value of r_0, indicating that absorption and emission transition moments are almost parallel. Nevertheless, very low values of $\langle r \rangle$ are measured for all of them. This

indicates ample movements during the excited-state lifetimes, which are in the ns domain for all the probes.

When rotation is hindered by friction force excerpted by the medium, the rotational correlation time, ϕ, is expressed by

$$\phi = \frac{f}{kT} \tag{2}$$

where f is the friction coefficient that is directly proportional to medium viscosity (η) and that depends on geometrical factors of the probe as well as on the boundary condition for the molecular rotation.

If medium friction is responsible for rotation retardation, ϕ should decrease with η/T, and $\langle r \rangle$ should decrease with temperature with an Arrhenius activation energy similar to the viscous flow. This is not observed for any probe. On the other hand, a totally restricted motion should show $\langle r \rangle = r_0$ and independent of T.

The independence of $\langle r \rangle$ with T points to a model of free rotation (not hindered by viscous friction) on a restricted space. This model also accounts for the fact that $\langle r \rangle$ is appreciably different from zero.

If the fluorescent probes are in an anisotropic environment, the anisotropy decays from a maximum value, r_0, to a stationary value, r_∞ after a certain period of time. This suggests that the molecule performs wobbling motions rather that free rotations [11].

To obtain an explicit expression for the time dependence of $r(t)$ it is necessary to assume a model for the dynamics of the probe. However, r_0 and r_∞ can be computed independently of any model in terms of the order parameter, S, defined by Saupe as

$$S = \langle P_2(\cos\theta) \rangle = \tfrac{3}{2} \left\langle \cos^2\theta \right\rangle - \tfrac{1}{2} \tag{3}$$

where P_2 is the second Legendre polynomial of the tilt angle of the orientation of the emission moment with respect to V. The angular brackets indicate an average over the excited-state population.

The Saupe order parameter determines the first nontrivial term in the series expansion of the orientation distribution function, $W(\theta)$, in term of Legendre polynomials:

$$W(\theta) = \sum_{l=0}^{\infty} \frac{4l+1}{4\pi} \langle P_{2l}(\cos\theta) \rangle \, P_{2l}(\cos\theta)$$
$$= \frac{1}{4\pi} + \frac{5}{4\pi} \langle P_2(\cos\theta) \rangle \, P_2(\cos\theta) + \cdots \tag{4}$$

The general expression for r_∞ when the chromophore can be modeled as a symmetric rotor, and either the absorption transition dipole moment or the emission transition dipole moment of the probe lies along its unique symmetry axis, $\hat{\mu}$, is [15]

$$r_\infty = r_0 \langle P_2(\cos\theta) \rangle^2 \tag{5}$$

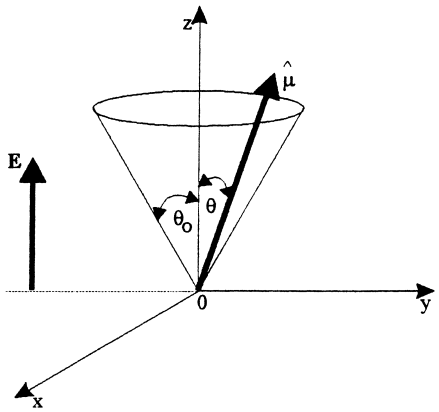

Fig. 4. Wobbling-in-cone model. $\hat{\mu}$ represents the symmetry axis of the chromophore, which forms an angle θ with the z-axis. The z-axis is coincident with the orientation of the linearly polarized E vector of the incident radiation (identical to the V direction defined in the text). There is unrestricted motion around the $\hat{\mu}$ axis which in turn wobbles around the z-axis within a cone of semiangle θ_0.

Thus, the order parameter provides model-independent information about the orientation distribution function at equilibrium

$$S^2 = \frac{r_\infty}{r_0} \tag{6}$$

An alternative interpretation is in terms of the wobbling-in-cone model [11,15], in which $\hat{\mu}$ can undergo free rotational diffusion within a cone of semiangle θ_0 (see Fig. 4) This corresponds to the normalized distribution:

$$W(\theta) = \begin{cases} (1/2\pi)(1-\cos\theta) & 0 \le \theta \le \theta_0 \\ 0 & \theta > \theta_0 \end{cases} \tag{7}$$

Using this distribution in Eq. (3) gives:

$$S = \langle P_2(\cos\theta) \rangle = \tfrac{1}{2}\cos\theta_0(1+\cos\theta_0) \tag{8}$$

which relates de model-independent Saupe order parameter with the cone semiangle defined in the wobbling-in-cone model.

If either the absorption transition dipole moment or the emission transition dipole moment of the probe is parallel to $\hat{\mu}$, combination of Eqs. (6) and (8) gives:

$$\frac{r_\infty}{r_0} = \left[\frac{1}{2}\cos\theta_0(1+\cos\theta_0) \right]^2 \tag{9}$$

The equilibrium distribution defined in Eq. (7) gives the following dependence of $r(t)$ [11]:

$$r(t) = r_\infty + (r_0 - r_\infty)\mathrm{e}^{-t/\phi_0} \tag{10}$$

Here ϕ_0 is the rotational correlation time in the limit of zero viscosity (free rotor reorientation time) which depends on the moment of inertia, I, and on temperature as [11]:

$$\phi_0 = \frac{2\pi}{9} \left(\frac{I}{kT} \right)^{1/2} \tag{11}$$

In a steady-state anisotropy experiment, the measured anisotropy is given by averaging $r(t)$ over the decay process. Using the distribution function defined in Eq. (7), one obtains:

$$\langle r \rangle = r_\infty + (r_0 - r_\infty)\frac{\phi_0}{\phi_0 + \tau} \quad (12)$$

where τ is the fluorescence lifetime. For luminescent molecules as the ones studied in this work, free rotor correlation times are in the order of some ps while fluorescence lifetimes are around some, ns so $\tau \gg \phi_0$ always. In this case the steady-state fluorescence anisotropy equals r_∞ (see Eq. (12)), and it is possible to obtain the Saupe order parameter from steady-state measurements.

All probes are adequately modeled by either prolate or oblate rotors [13,14] with transition dipole moments which coincide with the horizontal in plane direction. Values of $\langle r \rangle$, r_0, S, and θ_0 are listed in Table 1.

The fact that the measured anisotropy is temperature independent supports the assumption that rotation is not restricted by viscous forces, as it is found in solutions, but is limited by the environment. The values of S and θ_0 correlate with the size of the probe; Coumarin 153, the smallest of the three probes, gives the smallest order parameter (and hence the largest cone semiangle), while Rhodamine 101 gives the largest order parameter with the smallest cone semiangle.

Although we obtained a correlation between size and order parameter, there is not enough evidence to establish that the limitation in rotational motions is caused by a well-type potential imposed by the limited polymer free volume. Rotation may be also restricted by specific interactions between chromophores molecules and polymer units. Nevertheless, these interactions undoubtfully allow broad movements in the ns timescale of molecules embedded in the polymer network.

Acknowledgements

ML is a graduate fellow from UBA. PFA is a member of Carrera del Investigador Científico from CONICET (Research staff from Argentina National Research Council). The work was performed under financial support from UBA (EX-25) and Volkswagen Foundation (Germany).

References

[1] J.R. Lakowicz, Principles of Fluorescence Spectroscopy, Plenum Press, New York, 1983.
[2] J. Michl, E. Thulstrup, Spectroscopy with Polarized Light, VCH Publishers, New York, 1986.
[3] J.H. Nobbs, I.M. Ward, in: D. Phillips (Ed.), Polymer Photophysics, ch. 4, Chapman & Hall, London, 1995.
[4] L. Monnerie, in: D. Phillips (Ed.), Polymer Photophysics, ch. 6, Chapman & Hall, London, 1995.
[5] I. Soutar, C. Jones, D.M. Lucas, L. Swanson, J. Photochem. Photobiol. A: Chem. 102 (1996) 87.
[6] J.S. Royal, J.G. Victor, J.M. Torkelson, Macromolecules 25 (1992) 729.
[7] J.S. Royal, J.M. Torkelson, Macromolecules 25 (1992) 4792.
[8] J.S. Royal, J.M. Torkelson, Macromolecules 25 (1992) 1705.
[9] A. Akelah, A. Moet, Functionalized Polymers and their Applications, Chapman & Hall, London, 1990.
[10] J.L. Bourdelande, J. Font, Trends in Photochemistry and Photobiology 3 (1994) 481.
[11] A. Kawaski, Critic. Rev. Anal. Chem. 23 (1993) 459.
[12] A.P. Dorado, M.A. Llorente, I.F. Piérola, J. Photochem. Photobiol. A: Chem. 78 (1994) 193.
[13] M. Levitus, R.M. Negri, P.F. Aramendía, J. Phys. Chem. 99 (1995) 14231.
[14] M.-L. Horng, M.J.A. Gardecki, M. Maroncelli, J. Phys. Chem. A 101 (1997) 1030.
[15] A. Szabo, J. Chem. Phys. 81 (1984) 150.
[16] M.-L. Horng, M.J.A. Gardecki, M. Maroncelli, J. Phys. Chem. 99 (1995) 17311.
[17] T. Karstens, K. Kobs, J. Phys. Chem. 84 (1980) 1871.